An uncertain future change in aridity over the tropics

Monerie, P.-A. ORCID: https://orcid.org/0000-0002-5304-9559, Chadwick, R., Wilcox, L. J. ORCID: https://orcid.org/0000-0001-5691-1493 and Turner, A. G. ORCID: https://orcid.org/0000-0002-0642-6876 (2024) An uncertain future change in aridity over the tropics. Environmental Research Letters, 19 (5). 054048. ISSN 1748-9326 doi: https://doi.org/10.1088/1748-9326/ad42b8 Available at https://centaur.reading.ac.uk/116194/

ENVIRONMENTAL RESEARCH
LETTERS

LETTER • OPEN ACCESS

An uncertain future change in aridity over the tropics

To cite this article: Paul-Arthur Monerie *et al* 2024 *Environ. Res. Lett.* **19** 054048

ENVIRONMENTAL RESEARCH
LETTERS

OPEN ACCESS

RECEIVED
25 September 2023

REVISED
21 April 2024

ACCEPTED FOR PUBLICATION
24 April 2024

PUBLISHED
3 May 2024

LETTER

An uncertain future change in aridity over the tropics

Paul-Arthur Monerie[1,*], **Robin Chadwick**[2], **Laura J Wilcox**[1] and **Andrew G Turner**[1,3]

[1] National Centre for Atmospheric Science, Reading, United Kingdom
[2] Global Systems Institute, University of Exeter and Met Office Hadley Centre, Exeter, United Kingdom
[3] Department of Meteorology, University of Reading, Reading, United Kingdom
[*] Author to whom any correspondence should be addressed.

E-mail: p.monerie@reading.ac.uk, a.g.turner@reading.ac.uk, l.j.wilcox@reading.ac.uk and robin.chadwick@metoffice.gov.uk

Keywords: summer monsoon precipitation, aridity, climate change, greenhouse gases, anthropogenic aerosols, CMIP6

Supplementary material for this article is available online

Abstract

An ensemble of climate models from phase six of the Coupled Model Intercomparison Project shows that temperature and potential evapotranspiration (PET) are projected to increase globally towards the end of the 21st century. However, climate models show a spatially heterogeneous change in precipitation over the tropics. Consequently, future changes in aridity (a measure of water availability) are complex and location-dependent. We assess future changes in aridity using three climate models and several single-forcing experiments. Near-term (2021–2040) changes in aridity are small, and we focus instead on its long-term (2081–2100) changes. We show that the increase in greenhouse gases (GHG) primarily explains the spatial pattern, magnitude and ensemble spread of the long-term future changes in aridity. On this timescale, the effects of changes in emissions of anthropogenic aerosols are moderate compared to the effects of increases in atmospheric GHG concentrations. Model diversity in the responses to GHG concentration is large over northern Africa and North and South America. We suggest the large uncertainty is due to differences between models in simulating the effects of an increase in GHG concentrations on surface air temperature over the North Atlantic Ocean, on the interhemispheric temperature gradient, and on PET over North and South America.

1. Introduction

Anthropogenic activity has widespread effects on climate. Over the historical period, model evidence shows that the changes in greenhouse gas (GHG) concentrations and anthropogenic aerosol (AA) emissions have influenced recent variations in monsoon precipitation (Herman *et al* 2020, Hirasawa *et al* 2020, Marvel *et al* 2020, Monerie *et al* 2022, 2023), and temperature and potential evapotranspiration (PET) globally (Bonfils *et al* 2020). Anthropogenic activity has also led to anomalies in aridity, an indicator of potential water availability, whose changes are spatially heterogeneous (Bonfils *et al* 2020). An example of a consequence of the changes in precipitation in the monsoon regions is the drought of the Sahel (1970s–1980s) (Nicholson 2013), which led to famine and population migration. We expect those effects to strengthen in a warmer world, with GHG concentrations increasing (O'Neill *et al* 2016).

The future increase in GHG concentrations can lead to strong societal impacts, such as an increase in heat-related mortality (Mora *et al* 2017), risk of flooding (Hirabayashi *et al* 2013, Arnell and Gosling 2016), changes in monsoon precipitation (Chen *et al* 2020, Wang *et al* 2020) and drought risk (Ukkola *et al* 2020) over the tropics. Changes in emissions of AA affect future changes in regional temperature and monsoon precipitation, with substantial effects over Asia (Wilcox *et al* 2020). Future projections from the 5th and 6th phases of the Climate Model Intercomparison Project (CMIP5 and CMIP6, respectively) show that climate change has an effect on aridity, but that these changes are location-dependent (Greve and Seneviratne 2015, Greve *et al* 2019).

Around two-thirds of the world population is affected by the variability of summer monsoon precipitation (Wang and Ding 2006). Changes in land aridity will therefore have strong effects on societies in the monsoon regions, affecting, for instance,

agricultural yield and food security (Malpede and Percoco 2023), the occurrence of water shortage and desertification, as well as migration of people from affected areas. Understanding the future change in aridity is therefore societally important, particularly over areas that are vulnerable to climate change, such as the tropics. However, there are still large uncertainties in future changes in summer monsoon precipitation (Douville *et al* 2021) and aridity (Asadi Greve and Seneviratne 2015, Zarch *et al* 2017, Lian *et al* 2021).

Changes in aridity depend on changes in precipitation and evaporative demand, with both quantities associated with changes in surface air temperature, relative humidity, wind speed and available energy (Fu and Feng 2014). The uncertainty in the spatial pattern of the change in aridity is primarily due to the uncertainty in the change in precipitation (Lin *et al* 2015, Greve *et al* 2019) but the mechanisms at play still need be better understood. We fill this gap, assessing how future changes in different forcings (GHG, AA, and natural external forcing -NAT) may impact aridity over areas covered by the summer monsoon, how results could depend on a given representation of the climate system (model-dependence) and how changes in temperature gradients (and thus in atmospheric circulation) can lead to uncertainty at simulating the future change in aridity.

The paper is organized as follows: section 2 describes the simulations and methods we employ; section 3 describes the main results; section 4 discusses the results and section 5 concludes.

2. Data and method

2.1. Data

We assess the effects of climate change using models that participated in CMIP6, using the historical emission scenario (Eyring *et al* 2016), the SSP2-4.5 emission scenario (a low-medium emission scenario for which global mean radiative forcing is designed to reach 4.5 W m^{-2} at the end of the 21st century; O'Neill *et al* 2016), and single forcing experiments of the Detection and Attribution MIP (DAMIP; Gillett *et al* 2016). We used the SSP2-4.5 emission scenario which is the emission scenario that was used for the DAMIP simulations.

The single-forcing simulations are used to quantify the effects of each individual forcing on climate. In the single-forcing experiments all external forcings are kept constant at pre-industrial values, with the forcing of interest changing with time, following historical emissions from 1850 to 2020 and the SSP2-4.5 emission scenario thereafter:

- The AA-only simulations (hist-AER and SSP245-AER) resemble the historical and SSP2-4.5 simulations but are forced by changes in AA forcing only [black carbon, organic carbon, SO_2, SO_4, NO_x, NH_3, CO, non-methane volatile organic compounds (NMVOCs)]. Changes in AA emissions are heterogeneous, with for instance the emissions of SO_2 decreasing over the US, Europe, and China, and increasing over Africa and India (figure S1).
- The GHG-only simulations (hist-GHG and SSP245-GHG) resemble the historical and SSP2-4.5 simulations but are forced by changes in GHG only.
- The natural-only simulations (hist-NAT and SSP245-NAT) resemble the historical and SSP2-4.5 simulations but are forced with only solar and volcanic forcings.

We use the outputs of the three climate models that performed the future projections of the DAMIP experiments, and that provided at least 5 ensemble members to provide an estimation of the effect of internal climate variability and of the externally forced response. The number of models employed for future single-forcing comparisons is therefore limited by the lack of provision of suitable ensemble sizes by other modeling groups. We use 10 ensemble members each for CanESM5 and MIROC6 and 5 ensemble members for GISS-E2-1-G (table S1). All simulations are interpolated onto the same horizontal resolution, using a 2.5° regular grid for surface air temperature and precipitation.

We compare results of the three models we used here to an ensemble of 26 CMIP6 models, using the historical and SSP2-4.5 emission scenarios (table S2). The ensemble of the three climate models that provide future changes of the DAMIP experiments is hereafter called DAMIP, while the ensemble of the 26 CMIP6 models is hereafter called CMIP6.

2.2. Method

2.2.1. The climate moisture index (CMI) index

We use the CMI (Willmott and Feddema 1992), an indicator of the potential water availability, which was previously used to document climate change risks and changes in land aridity (e.g. Bonfils *et al* 2020). CMI depends on precipitation and PET and is calculated as follows:

$$\mathrm{CMI} = \begin{cases} \frac{P}{\mathrm{PET}} - 1 \text{ if } P < \mathrm{PET} \\ 1 - \frac{\mathrm{PET}}{P} \text{ if } P \geqslant \mathrm{PET} \end{cases},$$

where P is precipitation and PET. PET is calculated using the Penman–Monteith Equations following the Food and Agriculture Organization recommendations (Allen *et al* 1998) (see the method section of the supplementary material and table S3). An increase in atmospheric CO_2 concentration drives partial stomatal closure, reducing evapotranspiration (Lemaitre-Basset *et al* 2022). We then account for the effect of the vegetation response to an increase in CO_2 concentration, following Yang *et al*

(2019). See explanation in the supplementary material. Accounting for the vegetation response reduces the future change in PET but does not significantly affect the changes in aridity (figure S2).

CMI is calculated using monthly values prior to computing the seasonal mean. CMI ranges from −1 to +1, with positive values indicating a wet climate, which is when precipitation exceeds PET. CMI is positive during the monsoon season and is negative in winter. A negative value of CMI indicates a dry climate. A change in the value of the CMI will affect the probability of drought and water crisis—a change in sign is not required for a large societal impact.

2.2.2. The effect of external forcings

We follow the 6th assessment report of the Intergovernmental Panel on Climate Change and define a near-term projection as changes over the period 2021–2040, and long-term projections as changes occurring over 2081–2100, using the future emission scenarios, relative to the 1995–2014 reference period (Chen *et al* 2020).

The future effect of the change in GHG concentration is assessed using the hist-GHG and SSP245-GHG simulations and is hereafter framed as the GHG effect. The effect of the change in AA emissions (hereafter named the AA effect) is obtained using the hist-AER and SSP245-AER simulations. The effect of natural external forcing (hereafter named the NAT effect) is defined using the hist-NAT and SSP245-NAT simulations.

2.2.3. The monsoon domains

Monsoon domains are defined as containing grid points for which the annual range in precipitation May to September-November to March (MJJAS-NDJFM) exceeds an absolute value of 2.5 mm d^{-1} (Wang *et al* 2011) in observations Global Precipitation Climatology Centre (GPCC). Monsoon domains are named North America (NAM), South America (SAM), Northern Africa, Southern Africa (SAF), South Asia (SAS), East Asia (EAS) and Australia (AUS). The extent of the monsoon domains is model dependent (not shown), but Monerie *et al* (2022) show that changes in summer monsoon precipitation are not sensitive to the definition of the monsoon domain (e.g. using monsoon domains based on simulations rather than on observation).

2.2.4. Assessing robustness in the effects of the external forcings

We define the effects of the externally forced response as robust when the signal-to-noise ratio (S/N) is greater than one, with

$$S/N = \frac{\overline{\Delta v}}{\sigma_{\Delta v}}$$

where v is a given variable, Δv indicates the future change of v, the overbar denotes the ensemble mean and $\sigma_{\Delta v}$ is the standard deviation of the change of a given variable, computed across ensemble members. We assume that $\overline{\Delta v}$ is an estimate of the effects of the externally forced response because the ensemble mean removes the effects of internal variability that exists in each simulation but that are unlikely to be in phase (Deser *et al* 2014).

We compute S/N for each model separately, using all ensemble members (*e.g.* 10 ensemble members for CanESM5). For each model, $\sigma_{\Delta v}$ documents the deviation from the effects of the externally forced response, and we assume that it provides an estimate of the effects of internal variability. A S/N value greater than unity then indicates that the effects of the externally forced response exceed the estimate of the effects of internal climate variability, hence highlighting the robust effects of the externally forced response, relative to internal climate variability.

We also compute S/N using all available ensemble members together (i.e. 35 ensemble members, with 10 from CanESM5, 5 from GISS-E2-1-G, and 10 from MIROC6). When computed from the ensemble members of all models, an S/N value greater than unity indicates that the estimate of the externally forced response is greater than the combination of the model uncertainty and the effects of internal climate variability.

In addition to the S/N ratio we quantified the significance of the anomalies using a Student's t test. We show that the quantification of the robustness of the results is only moderately impacted by the metric we use (figures S3 and S4).

2.2.5. The indices

We define the latitudinal location of the intertropical convergence zone (ITCZ) as the center of mass of the zonal mean of the precipitation, averaged across all longitudes and measured between 30° S and 30° N (Monerie *et al* 2023). The intertropical temperature difference (ITD) is defined as the difference in surface air temperature, between the northern [0–40° N] and southern [0-40° S] tropical mean, considering ocean grid points only, following Cao *et al* (2020).

We define a North Atlantic [0–60° N; 70° W–0] minus South Atlantic [60° S–0; 70° W–10° E] temperature gradient (hereafter named NA/SA) to follow Hoerling *et al* (2006). We also account for land temperature using a land-sea temperature contrast, defined as the difference between the surface-air temperatures of northern Africa (over Sahara) [15° N–30° N; 10° E–30° E] and the South Atlantic Ocean [30° S–0; 70° W–10° E] (SAH/SA), which is a known driver of northern African precipitation (Jin *et al* 2020).

3. Results

In section 3 we assess the effects of the external forcings on aridity, temperature, and precipitation,

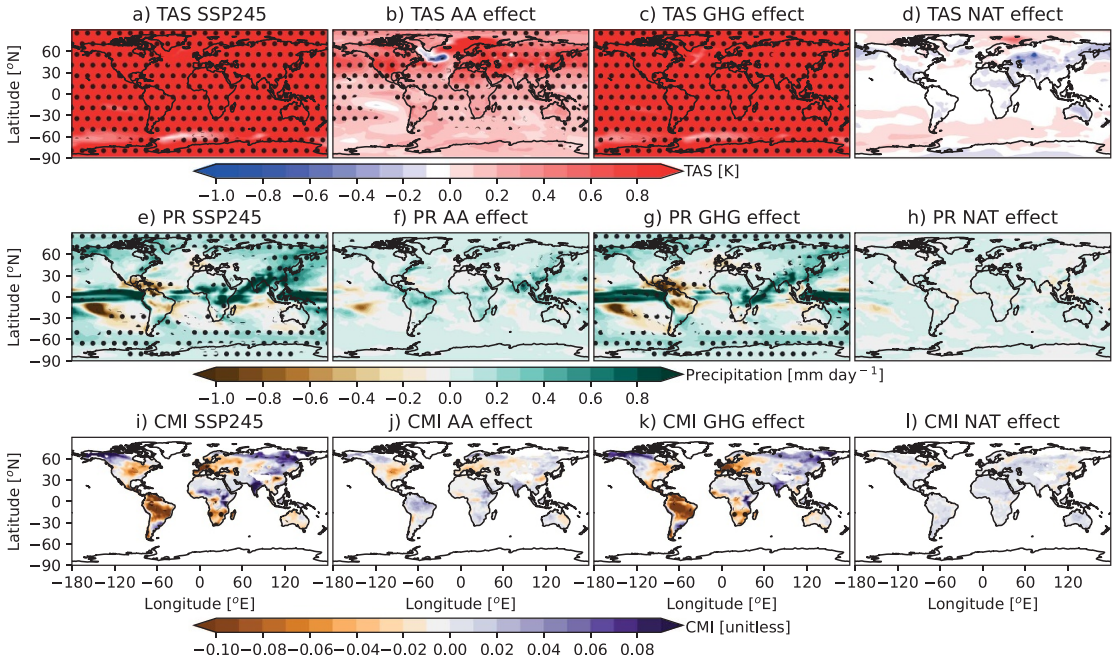

Figure 1. DAMIP ensemble-mean from the single-forcing ensemble of the long-term projections of changes in (a)–(d) surface air temperature (in K), (e)–(h) precipitation (in mm d^{-1}) (middle panel) and (i)–(l) CMI [unitless], as defined by the difference between the future period 2081–2100 and the 1995–2014 period (see Method). Effects of (a) (e) (i) all external forcing, and the (b) (f) (j) AA effect, the (c) (g) (k) GHG effect and the (d) (h) (l) NAT effects. Stippling indicates robustness in the result, as defined when the signal-to-noise ratio is greater than unity (see Method). Changes are shown for the warm season, in MJJAS over the Northern Hemisphere, and in NDJFM over the Southern Hemisphere.

focusing on the ensemble means and on each individual external forcing (section 3.1), and each individual DAMIP model (sections 3.2 and 3.3). We investigate mechanisms that explain differences between climate models at simulating the changes in aridity in section 3.4.

3.1. The effects of anthropogenic external forcing on surface air temperature, precipitation, and aridity

Surface air temperature is expected to increase towards the end of the 21st century due to anthropogenic activity (figure 1(a)). The DAMIP experiments show that the increase in global mean surface air temperature (GMST) is primarily driven by increasing GHG concentrations (figure 1(c)). The AA effect also contributes to the increase in GMST (figure 1(b)) through allowing an increase in surface downwelling shortwave radiation as aerosol emissions reduce (figures S1 and S5). The increase in surface air temperature due to aerosol reductions is robust almost everywhere, except over the North Atlantic subpolar gyre. Here, the change in surface air temperature is uncertain, as seen in Lehner *et al* (2020), and which we hypothesize to be due to changes of the oceanic circulation (Bellomo *et al* 2021). We show that PET increases, globally, in a warmer climate, consistent with the literature (e.g. Greve *et al* 2019) (figure S6).

Changes in regional precipitation are more uncertain than changes in surface air temperature, as shown by there being fewer regions of the globe where S/N values exceed unity (figures 1(a) and (e)). Precipitation increases over the tropics, with the exception of central and SAM, where precipitation decreases due to the externally forced response (figure 1(e)), in agreement with Chen *et al* (2020). Changes in precipitation are primarily contributed by the GHG effect (figure 1(g)). Changes in aerosol emissions over the 21st century are associated with an increase in precipitation over the tropics, but with low robustness across the ensemble (figure 1(f)).

Changes in the CMI index follow the change in precipitation and are more uncertain than the changes in surface air temperature (figures 1(a) and (i)). The central Sahel and India are projected to become wetter, while aridity increases over central and SAM, western Sahel, southern Africa, and East and Southeast Asia (Figure i), in agreement with previous studies (Asadi Greve and Seneviratne 2015, Zarch *et al* 2017, Greve *et al* 2019). Like precipitation, the change in CMI is primarily contributed by the GHG effect (figure 1(k)), while the AA effect is weaker over the monsoon regions in the long term (figure 1(j)).

In contrast to the GHG and AA effects, NAT effects do not contribute to the change in surface air temperature (figure 1(d)), precipitation (figure 1(h)), and aridity (figure 1(l)).

We expect the relative importance of the GHG and AA effects on the full change in aridity to be dependent on the timescale of interest. We show that

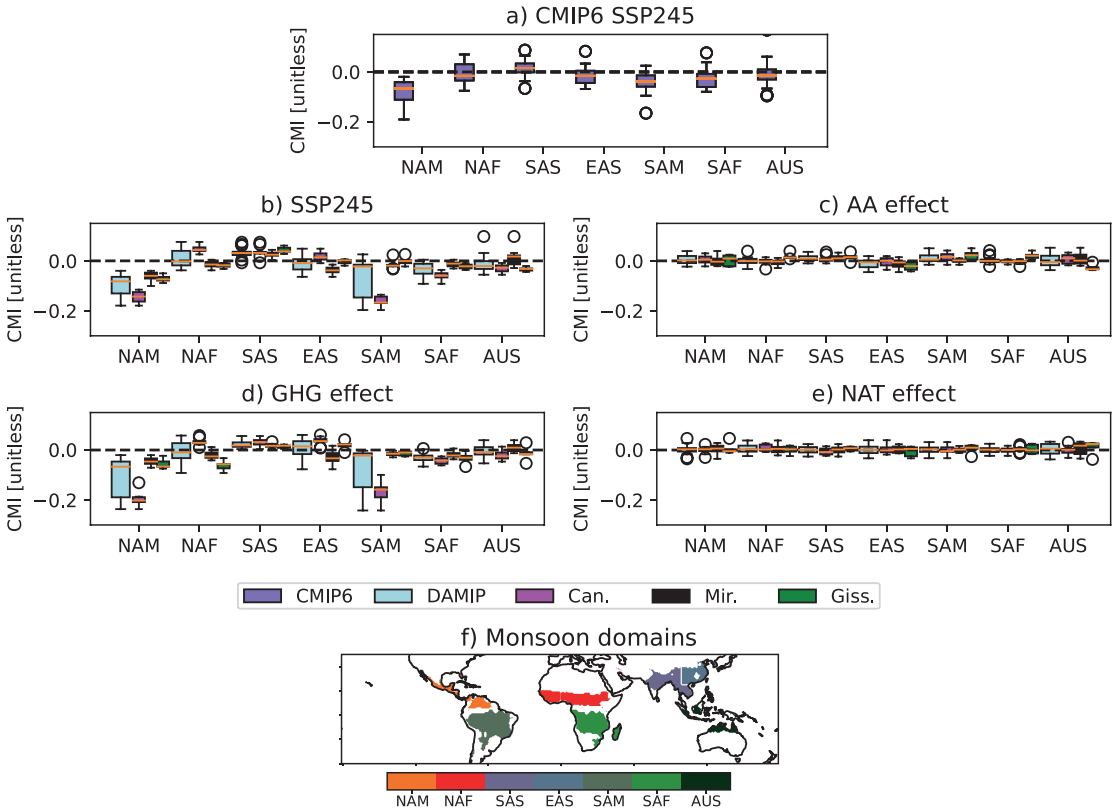

Figure 2. Box plot of the long-term changes in aridity index (CMI index) [unitless] averaged over each monsoon domain. Results are given for the effects of all external forcing (SSP2-4.5 minus historical) derived from (a) CMIP6 (in purple). Results are also given for the DAMIP ensemble (pale blue) and for each climate model: CanESM5 (magenta), MIROC6 (black) and GISS-E2-1-G (green), and for the (b) effect of all external forcing, for the (c) AA effect, (d) GHG effect, and (e) NAT effect. Box plots show the median value (orange vertical line), the first and third quartile and the minimum and maximum value, and the outliers (black circles). Changes are shown for the warm season, in MJJAS over the Northern Hemisphere, and in NDJFM over the Southern Hemisphere. The monsoon domains that were used to compute the averages are shown within panel f. Please see the historical and future values of CMI that are used for panels (b) and (d) in figure S14.

the AA effect is greater than the GHG effect over the Sahel for the near-term horizon (2021–2040), and of the same importance as the GHG effect over India (figure S7). However, changes in aridity are small globally for the near-term horizon (figure S8), with fewer regions in which S/N exceeds unity (figure S7). Therefore, we focus the remaining analysis on the long-term change in aridity.

3.2. Model and monsoon-domain dependence of aridity changes

We show changes in CMI, averaged over each monsoon domain and in response to changes of all forcings (figure 2), for long-term projections, and for both CMIP6 and DAMIP ensembles. The CMIP6 ensemble projects an increase in aridity over the NAM, SAM, SAF and AUS monsoon domains, with a wetter climate over the SAS monsoon domain and with no change over the NAF and EAS monsoon regions (figure 2(a)). The DAMIP ensemble shows the same behavior in changes in aridity (figure 2(b)), showing that it provides a good representation of the CMIP6 ensemble. There is a large diversity of responses among the three climate models, both in terms of magnitude (e.g. for the SAM summer monsoon precipitation) and sign of the change (e.g. NAF summer monsoon precipitation). The strongest differences between models are obtained over the NAM, SAM, and NAF monsoon domains, and for the EAS monsoon domain (figure 2(b)).

CanESM5 is the most sensitive to GHG, simulating the strongest changes in aridity relative to the CMIP6 ensemble (figures 2(a) and (b)). We show this to not solely due to a greater warming in CanESM5, as scaling the changes in aridity by changes in GMST does not alter the results (figure S9). We thus suggest that one relevant explanation for the differences between climate models at simulating the changes in CMI is the difference in the patterns of change in surface air temperature and atmospheric circulation.

The AA effect is associated with a small change in the CMI, and the ensemble spread is low (figure 2(c)). In contrast, GHG effects largely explain the future change and ensemble spread in the aridity index (figure 2(d)). The NAT effect does not lead to robust changes in aridity over the monsoon domains (figure 2(e)), consistent with results of figure 1, because of the considered time scale (20 years) and because there are no strong changes in the solar forcing and the volcanic emissions. The same

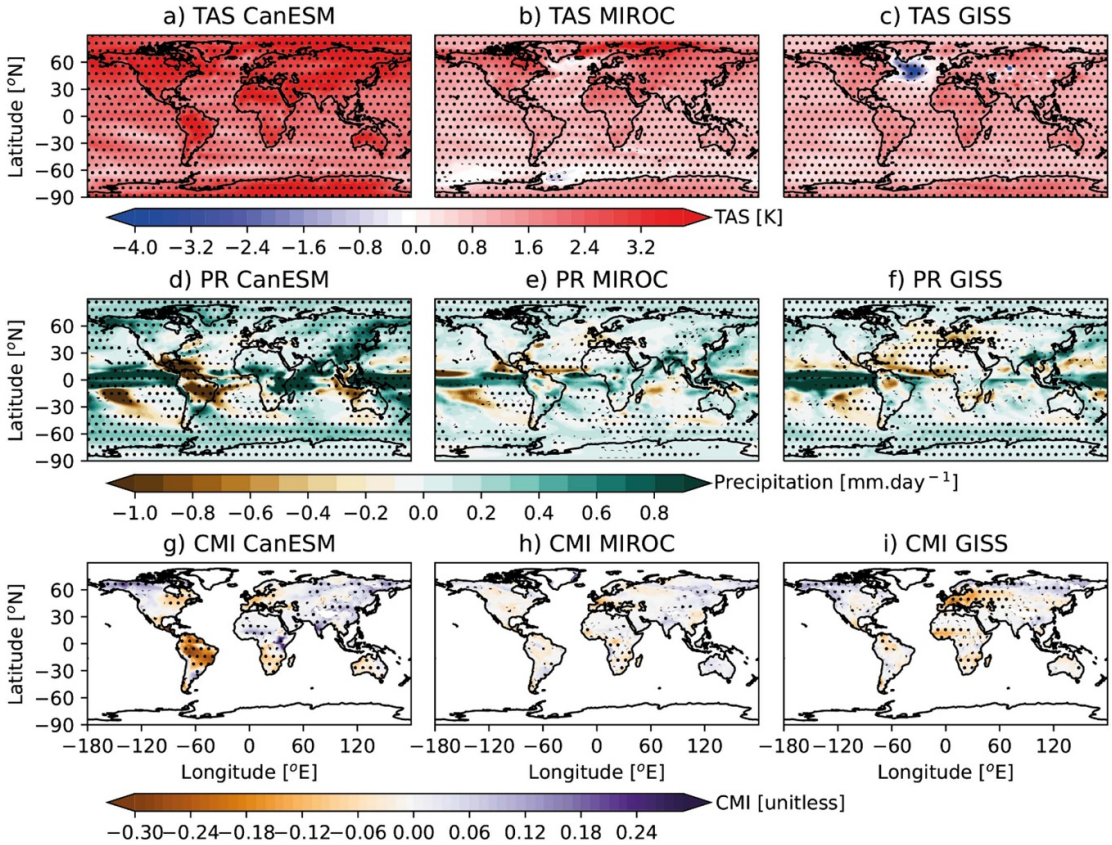

Figure 3. Long-term projection of the GHG effect on (a)–(c) surface air temperature (in K), (d)–(f) precipitation (in mm d^{-1}) and (g)–(i) CMI [unitless], as defined by the difference between the future period 2081–2100 and the 1995–2014 period (see method). Results are given for the ensemble-mean of (left row) CanESM5, (middle row) MIROC6 and (right row) GISS-E2-1-G. Stippling indicates robustness in the result, as defined when the signal-to-noise ratio is greater than unity (see method). Changes are shown for the warm season, in MJJAS over the Northern Hemisphere, and in NDJFM over the Southern Hemisphere.

conclusion also holds for the near-term horizon (figure S8), with strong differences between climate models primarily arising due to the GHG effect.

3.3. Model differences in simulating the GHG effect

The GHG effect explains the differences between models in simulating the long-term change in aridity. Thus, we focus on GHG effects on surface air temperature, precipitation, and aridity in each model. We focus on the long-term projection to capture the largest possible externally forced signal.

CanESM5 simulates a stronger increase in GMST and a stronger land-ocean thermal contrast than MIROC6 and GISS-E2-1-G (figures 3(a)–(c)). More specifically, a striking difference is obtained over the extratropical North Atlantic Ocean, with CanESM5 simulating a strong and robust warming, MIROC6 simulating a weaker warming, and GISS-E2-1-G simulating a robust cooling of the extratropical North Atlantic (figures 3(a)–(c)).

CanESM5 also simulates stronger changes in precipitation than the other models globally (figures 3(d)–(f)). Strong differences are obtained regionally, with CanESM5 producing a strong robust decrease in precipitation over central and SAM, while changes are moderate and not robust in MIROC6 and GISS-E2-1-G (figures 3(d)–(f)). Models show a large diversity in response over northern Africa, with CanESM5 simulating a robust increase in precipitation, MIROC6 simulating a zonal contrast with a decrease in precipitation over the central Sahel and an increase over the western Sahel, as seen in a majority of CMIP5 and CMIP6 models (Monerie *et al* 2020), and GISS-E2-1-G producing a large-scale decrease in precipitation (figure 3(f)). There is more consistency in the sign of change over eastern India.

The change in aridity (figures 3(g) and (i)) follows the change in precipitation (figures 3(d)–(f)) over the monsoon regions, showing a divergence between models at projecting the long-term change in aridity, and suggesting that the change in precipitation controls the change in aridity.

3.4. Mechanisms

We now assess mechanisms that explain the differences between climate models at simulating the GHG effect on aridity over land.

Precipitation increases over most of the monsoon domains and decreases over the NAM and SAM monsoon domains (figure 4(a)). Unlike precipitation, PET increases globally (figure 4(b)). The ensemble spread is higher for the change in precipitation than in PET,

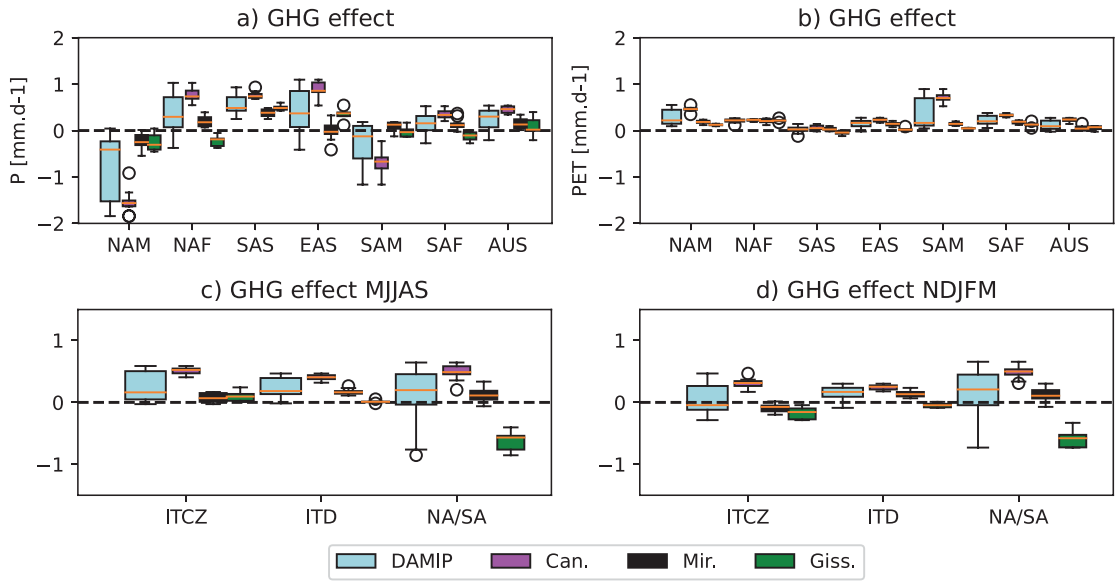

Figure 4. Box plot of the GHG effect on long term projection of (a) precipitation and (b) the potential evapotranspiration (in mm d^{-1}) averaged over each monsoon domain and for the summer period. Long term changes of the meridional location of the ITCZ [°N], of the ITD [K] and the NA/SA temperature gradient [K], in (c) MJJAS and (d) NDJFM. Results are given for the DAMIP ensemble (in pale blue) and for each model (CanESM5 in magenta, MIROC6 in black and GISS-E2-1-G in green). Box plots show the median value (orange vertical line), the first and third quartile and the minimum and maximum value.

consistent with figure 3, suggesting that the change in precipitation explains the uncertainty at simulating the change in aridity. The ensemble spread is high though for the change in PET over the NAM and SAM monsoon regions (figure 4(b)), suggesting that the differences between models at simulating PET contribute to the uncertainty in the change in aridity (figure 2(b)). However, comparison of the magnitude of the ensemble-spread of the change in precipitation and PET shows that the key for understanding the future change in aridity lies in the future change in precipitation. We then focus the analysis on known drivers of summer monsoon precipitation change. Following section 3.3 we focus the analysis on the GHG effect.

We first focus on a large-scale picture of the monsoons, tracking the meridional shift of the ITCZ and the large-scale temperature gradient. The ITCZ shifts northward in both MJJAS (figure 4(c)) and NDJFM (figure 4(d)), consistent with a strengthening of the ITD (Cao *et al* 2020). These large-scale changes are consistent with the changes of monsoon precipitation, locally, with a northward shift of the ITCZ associated with an increase in precipitation over the NAF, SAS and EAS monsoon domains, and with a decrease in precipitation over the NAM and SAM monsoon domains. Besides, the more pronounced change in ITD and location of the ITCZ in CanESM5 than in the other models is consistent with the stronger changes in precipitation in that model.

In addition to the large-scale temperature gradient, we show the change of the cross-equatorial Atlantic temperature gradient (NA/SA; figures 4(c) and (d)), both having effects on West African (Hoerling *et al* 2006, He *et al* 2023) and South American monsoon precipitation (Joetzjer *et al* 2013, Wang *et al* 2020). The change of the NA/SA temperature gradient is model dependent, with CanESM5 projecting a strengthened cross-equatorial Atlantic temperature gradient while GISS-E2-1-G projects a weakening of the NA/SA temperature gradient. This is consistent with the change in NAF monsoon precipitation, positive in CanESM5 and negative in GISS-E2-1-G. MIROC6 produces a moderate change of both NAF precipitation and NA/SA temperature gradient. This relationship between NA/SA and NAF precipitation is also obtained with the larger CMIP6 ensemble (full response to climate change), with a correlation coefficient between both indices of $r = 0.76$. These results therefore reveal a strong control of the change in subtropical North Atlantic temperature on future changes in West African precipitation and aridity.

In addition to the ocean temperature, the SAH/SA temperature gradient also strengthens more strongly in CanESM5 than in the other models (not shown), potentially indicating a strong effect of differences in land warming on the NAF summer monsoon precipitation, as shown in Hall and Peyrillé (2006), among others.

Changes in summer monsoon precipitation are also associated with changes in Pacific SSTs (e.g. ENSO, Pacific Decadal Oscillation), globally. Here, we show that the tropical Pacific warms more in CanESM5 than in GISS-E2-1-G and MIROC6 (figures 3(a)–(c)), but we found no evidence showing that changes in the Pacific temperature gradients (e.g. the equatorial Pacific zonal temperature gradient; Watanabe *et al* 2021) could explain the differences

we show between models at simulating the future change in summer monsoon precipitation and aridity (figure S10).

4. Discussion

We show a large uncertainty in projected changes of the Atlantic subpolar gyre temperature (figures 3(a)–(c)), which we suggest has a strong bearing on the uncertainty in projected changes in the Atlantic cross-equatorial temperature gradient, NAF precipitation and aridity. We show that CanESM5, which projects an increase in the Atlantic subpolar gyre temperature, simulates a small weakening of the atlantic meridional overturning circulation (AMOC) (figure S11). On the contrary, GISS-E2-1-G simulates a weakening of the NA/SA temperature gradient and an increase in aridity over northern Africa, in line with an abrupt decline of the AMOC (figure S11). This is consistent with Baker *et al* (2023), who show that changes in the AMOC are weak for CanESM5 and strong for GISS-E2-1-G, and with MIROC6 showing a change in the AMOC that is in the middle of the CMIP6 distribution. We thus suggest that the GHG effects on the future change of the AMOC explain a large part of the uncertainty for future change of NAF aridity, following the results of Bellomo *et al* (2021) and Swingedouw *et al* (2021).

Beyond changes in temperature gradients and subsequent changes in atmospheric circulation, we find that changes in aridity are associated with changes in soil moisture (upper 10 cm) over the tropics (e.g. the spatial pattern correlation is $r = 0.73$ in CanESM5, r = 0.74 in MIROC6 and $r = 0.68$ in GISS-E2-1-G). This shows that there are strong feedbacks between changes in PET and soil moisture (Seneviratne *et al* 2010), also suggesting that differences between models at simulating land-atmosphere feedbacks could explain a proportion of the difference we show between projections of different climate models. This was shown to be particularly relevant for South American precipitation (Baker *et al* 2021), where differences between models at simulating land-atmosphere feedbacks can shape future changes in precipitation.

We show that uncertainty at simulating the future change of PET is particularly high over northern and southern America. We did not analyze the sources of uncertainty for the change of PET due to limitations in the data availability. However, further analysis of the change in leaf-area index, and quantification of the effects of the direct (a high CO_2 concentration leads to partial stomatal closure) and indirect (a high CO_2 concentration is associated with a higher atmospheric vapor pressure deficit) effect of CO_2 would allow better understanding of the uncertainty in changes in PET and aridity. For example, we show significant future changes in leaf area index in CanESM5 (figure S12), which may affect PET and contribute to uncertainty in simulating future changes in aridity.

5. Conclusion

Future changes in aridity have strong societal impacts, through effects on human health, water availability and agricultural yield. A large-ensemble analysis shows that the effects of climate change can result in a less arid climate over South Asia and increasingly arid conditions over Central America, South America, and southern Africa. No significant changes in aridity are found over northern Africa and East Asia for the ensemble mean. We show that changes in aridity are model dependent and monsoon-domain dependent.

We analyzed the effects of individual anthropogenic external forcings on future changes in aridity, for the first time, and with a focus on monsoon precipitation, using the single-forcing DAMIP experiments (Gillett *et al* 2016). We show that the uncertainty in changes in aridity is shaped by the uncertain response to an increase in atmospheric greenhouse concentrations (the GHG effect). The strongest differences between model responses to the GHG effect concern the changes in precipitation and aridity over Central and South America, West Africa, and East Asia. We suggest this to be due to differences at simulating the changes in the interhemispheric and cross-Atlantic temperature gradients, which subsequently have effects on atmospheric circulation and precipitation.

Differences between models at simulating the effect of AAs are a major source of uncertainty for simulating changes for the GMST (Boucher *et al* 2013), and this uncertainty is greater at regional scales. The differences between models at simulating the effects of AAs could potentially yield strong uncertainty in the change in monsoon precipitation (Shonk *et al* 2020, Monerie *et al* 2022, 2023) and aridity (Chai *et al* 2021), and could explain a large part of the precipitation change uncertainty in near-term and long-term changes in monsoon precipitation and aridity. However, the three climate models we employ here simulate similar, relatively small, changes in monsoon precipitation and aridity due to the future reductions in AA emissions. The inter-model spread in monsoon precipitation and aridity due to AA effects is therefore low for the end of the 21st century. Uncertainty in the AA effect on monsoon precipitation is however as high as the uncertainty for the GHG effect for the near-term change and for several specific monsoon domains. We suggest these results might depend on the models we analyze and that an increased number of models could yield more informative results.

We show the future change in precipitation and aridity to be model-dependent over most of the monsoon domains for both near-future and long-term time horizons. This could lead to divergence between models in the estimated time of emergence (*e.g.* figure S13), a key metric of interest for decision makers. In addition, Douville and Willett (2023) show that future drying could be stronger than simulated by climate models, affecting mitigation and adaptation strategies.

Data availability statement

The data that support the findings of this study are openly available at the following URL/DOI: https://esgf-index1.ceda.ac.uk/search/cmip6-ceda/. DOIS/URLs of each of the historical, SSP2-4.5, Hist-aer, Hist-nat, Hist-GHG, SSP2-4.5-aer, SSP2-4.5-nat and SSP2-4.5-GHG simulations are respectively, for CanESM5: doi: https://doi.org/10.22033/ESGF/CMIP6.3610, doi: https://doi.org/10.22033/ESGF/CMIP6.3685, doi: https://doi.org/10.22033/ESGF/CMIP6.3597, doi: https://doi.org/10.22033/ESGF/CMIP6.3601, doi: https://doi.org/10.22033/ESGF/CMIP6.3596, doi: https://doi.org/10.22033/ESGF/CMIP6.3687, doi: https://doi.org/10.22033/ESGF/CMIP6.3688, doi: https://doi.org/10.22033/ESGF/CMIP6.3686, for MIROC6: doi: https://doi.org/10.22033/ESGF/CMIP6.5603, doi: https://doi.org/10.22033/ESGF/CMIP6.5746, doi: https://doi.org/10.22033/ESGF/CMIP6.5579, doi: https://doi.org/10.22033/ESGF/CMIP6.5583, doi: https://doi.org/10.22033/ESGF/CMIP6.5578, doi: https://doi.org/10.22033/ESGF/CMIP6.5748, doi: https://doi.org/10.22033/ESGF/CMIP6.5749, doi: https://doi.org/10.22033/ESGF/CMIP6.5747, and GISS-E2-1-G: doi: https://doi.org/10.22033/ESGF/CMIP6.7127, doi: https://doi.org/10.22033/ESGF/CMIP6.7415, doi: https://doi.org/10.22033/ESGF/CMIP6.7081, doi: https://doi.org/10.22033/ESGF/CMIP6.7089, doi: https://doi.org/10.22033/ESGF/CMIP6.7079, doi: https://doi.org/10.22033/ESGF/CMIP6.7420, doi: https://doi.org/10.22033/ESGF/CMIP6.7422, doi: https://doi.org/10.22033/ESGF/CMIP6.7418.

Acknowledgments

A G T is supported by the National Centre for Atmospheric Science through the NERC National Capability International Programmes Award (NE/X006263/1) and the TerraFIRMA project (NE/W004895/1). L J W acknowledges funding by the Research Council of Norway through Grant No. 324182 (CATHY) and the Natural Environment Research Council (NERC; Grant NE/W004895/1, TerraFIRMA). R C was supported by the Newton Fund through the Met Office Climate Science for Service Partnership Brazil (CSSP Brazil). We acknowledge the World Climate Research Programme's Working Group on Coupled Modelling, which is responsible for CMIP, and we thank the climate modelling groups for producing and making available their model output. For CMIP the U.S. Department of Energy's Program for Climate Model Diagnosis and Intercomparison provides coordinating support and led development of software infrastructure in partnership with the Global Organization for Earth System Science Portals. We also thank the three anonymous reviewers for their comments and suggestions.

ORCID iDs

Paul-Arthur Monerie https://orcid.org/0000-0002-5304-9559
Robin Chadwick https://orcid.org/0000-0001-6767-5414
Laura J Wilcox https://orcid.org/0000-0001-5691-1493
Andrew G Turner https://orcid.org/0000-0002-0642-6876

References

Allen R G, Pereira L S, Raes D and Smith M 1998 Crop evapotranspiration-guidelines for computing crop water requirements-FAO irrigation and drainage paper 56 *Fao, Rome* **300** D05109 (available at: https://sorbonne-universite.primo.exlibrisgroup.com/discovery/openurl?institution=33BSU_INST&vid=33BSU_INST:33BSU&rft.aulast=Allen&rft.aulast=Pereira&rft.aulast=Raes&rft.aulast=Smith&url_ver=Z39.88-2004&rft.date=1998&rfr_id=info:sid%2Fwiley&rft.genre=other&rft.aufirst=R.%20G.&rft.aufirst=L.%20S.&rft.aufirst=D.&rft.aufirst=M.&rft.title=Crop%20evapotranspiration%3Fguidelines%20for%20computing%20crop%20water%20requirements%3FFAO%20irrigation%20and%20drainage%20paper%2056)

Arnell N W and Gosling S N 2016 The impacts of climate change on river flood risk at the global scale *Clim. Change* **134** 387–401

Baker J A, Bell M J, Jackson L C, Renshaw R, Vallis G K, Watson A J and Wood R A 2023 Overturning pathways control AMOC weakening in CMIP6 models *Geophys. Res. Lett.* **50** e2023GL103381

Baker J C, Garcia-Carreras L, Buermann W, De Souza D C, Marsham J H, Kubota P Y, Gloor M, Coelho C A and Spracklen D V 2021 Robust amazon precipitation projections in climate models that capture realistic land–atmosphere interactions *Environ. Res. Lett.* **16** 74002

Bellomo K, Angeloni M, Corti S and von Hardenberg J 2021 Future climate change shaped by inter-model differences in atlantic meridional overturning circulation response *Nat. Commun.* **12** 3659

Bonfils C J, Santer B D, Fyfe J C, Marvel K, Phillips T J and Zimmerman S R 2020 Human influence on joint changes in temperature, rainfall and continental aridity *Nat. Clim. Change* **10** 726–31

Boucher O *et al* 2013 *Climate Change 2013: The Physical Science Basis. Contribution of Working Group I to the Fifth Assessment Report of the Intergovernmental Panel on Climate Change* ed K Tignor *et al* (Cambridge University Press)

Cao J, Wang B, Wang B, Zhao H, Wang C and Han Y 2020 Sources of the intermodel spread in projected global monsoon

hydrological sensitivity *Geophys. Res. Lett.* **47** e2020GL089560
Chai R, Mao J, Chen H, Wang Y, Shi X, Jin M, Zhao T, Hoffman F M, Ricciuto D M and Wullschleger S D 2021 Human-caused long-term changes in global aridity *npj Clim. Atmos. Sci.* **4** 65
Chen Z, Zhou T, Zhang L, Chen X, Zhang W and Jiang J 2020 Global land monsoon precipitation changes in CMIP6 projections *Geophys. Res. Lett.* **47** e2019GL086902
Deser C, Phillips A S, Alexander M A and Smoliak B V 2014 Projecting north american climate over the next 50 years: uncertainty due to internal variability *J. Clim.* **27** 2271–96
Douville H *et al* 2021 Water cycle changes
Douville H and Willett K M 2023 A drier than expected future, supported by near-surface relative humidity observations *Sci. Adv.* **9** eade6253
Eyring V, Bony S, Meehl G A, Senior C A, Stevens B, Stouffer R J and Taylor K E 2016 Overview of the coupled model intercomparison project phase 6 (CMIP6) experimental design and organization *Geosci. Model. Dev.* **9** 1937–58
Fu Q and Feng S 2014 Responses of terrestrial aridity to global warming *J. Geophys. Res. Atmos.* **119** 7863–75
Gillett N P, Shiogama H, Funke B, Hegerl G, Knutti R, Matthes K, Santer B D, Stone D and Tebaldi C 2016 The detection and attribution model intercomparison project (DAMIP∼v1.0) contribution to CMIP6 *Geosci. Model. Dev.* **9** 3685–97
Greve P, Roderick M L, Ukkola A M and Wada Y 2019 The aridity index under global warming *Environ. Res. Lett.* **14** 124006
Greve P and Seneviratne S I 2015 Assessment of future changes in water availability and aridity *Geophys. Res. Lett.* **42** 5493–9
Hall N M and Peyrillé P 2006 Dynamics of the West African monsoon *J. Phys. IV (Proc.)* **139** 81–99
He C, Clement A C, Kramer S M, Cane M A, Klavans J M, Fenske T M and Murphy L N 2023 Tropical atlantic multidecadal variability is dominated by external forcing *Nature* **622** 521–7
Herman R J, Giannini A, Biasutti M and Kushnir Y 2020 The effects of anthropogenic and volcanic aerosols and greenhouse gases on twentieth century sahel precipitation *Sci. Rep.* **10** 12203
Hirabayashi Y, Mahendran R, Koirala S, Konoshima L, Yamazaki D, Watanabe S, Kim H and Kanae S 2013 Global flood risk under climate change *Nat. Clim. Change* **3** 816–21
Hirasawa H, Kushner P J, Sigmond M, Fyfe J and Deser C 2020 Anthropogenic aerosols dominate forced multidecadal sahel precipitation change through distinct atmospheric and oceanic drivers *J. Clim.* **33** 1–56
Hoerling M, Hurrell J, Eischeid J and Phillips A 2006 Detection and attribution of twentieth-century northern and southern african rainfall change *J. Clim.* **19** 3989–4008
Jin C, Wang B and Liu J 2020 Future changes and controlling factors of the eight regional monsoons projected by CMIP6 models *J. Clim.* **33** 9307–26
Joetzjer E, Douville H, Delire C and Ciais P 2013 Present-day and future amazonian precipitation in global climate models: CMIP5 versus CMIP3 *Clim. Dyn.* **41** 2921–36
Lehner F, Deser C, Maher N, Marotzke J, Fischer E M, Brunner L, Knutti R and Hawkins E 2020 Partitioning climate projection uncertainty with multiple large ensembles and CMIP5/6 *Earth Syst. Dyn.* **11** 491–508
Lemaitre-Basset T, Oudin L and Thirel G 2022 Evapotranspiration in hydrological models under rising CO_2: a jump into the unknown *Clim. Change* **172** 36
Lian X *et al* 2021 Multifaceted characteristics of dryland aridity changes in a warming world *Nat. Rev. Earth Environ.* **2** 232–50
Lin L, Gettelman A, Feng S and Fu Q 2015 Simulated climatology and evolution of aridity in the 21st century *J. Geophys. Res. Atmos.* **120** 5795–815
Malpede M and Percoco M 2023 Aridification, precipitations and crop productivity: evidence from the aridity index *Europ. Rev. Agric. Econ.* **50** 978–1012
Marvel K, Biasutti M and Bonfils C 2020 Fingerprints of external forcing agents on sahel rainfall: aerosols, greenhouse gases, and model-observation discrepancies *Environ. Res. Lett.* **15** 084023
Monerie P A, Dittus A J, Wilcox L J and Turner A G 2023 Uncertainty in simulating twentieth century West African precipitation trends: the role of anthropogenic aerosol emissions *Earth's Future* **11** e2022EF002995
Monerie P A, Wainwright C M, Sidibe M and Akinsanola A A 2020 Model uncertainties in climate change impacts on sahel precipitation in ensembles of CMIP5 and CMIP6 simulations *Clim. Dyn.* **55** 1385–401
Monerie P A, Wilcox L J and Turner A G 2022 Effects of anthropogenic aerosol and greenhouse gas emissions on northern hemisphere monsoon precipitation: mechanisms and uncertainty *J. Clim.* **35** 1–66
Mora C *et al* 2017 Global risk of deadly heat *Nat. Clim. Change* **7** 501–6
Nicholson S E 2013 The west african sahel: a review of recent studies on the rainfall regime and its interannual variability *ISRN Meteorology* **2013** 1–32
O'Neill B C *et al* 2016 The scenario model intercomparison project (ScenarioMIP) for CMIP6 *Geosci. Model. Dev.* **9** 3461–82
Seneviratne S I, Corti T, Davin E L, Hirschi M, Jaeger E B, Lehner I, Orlowsky B and Teuling A J 2010 Investigating soil moisture–climate interactions in a changing climate: a review *Earth Sci. Rev.* **99** 125–61
Shonk J K, Turner A G, Chevuturi A, Wilcox L J, Dittus A J and Hawkins E 2020 Uncertainty in aerosol radiative forcing impacts the simulated global monsoon in the 20th century *Atmos. Chem. Phys.* **20** 14903–15
Swingedouw D, Bily A, Esquerdo C, Borchert L F, Sgubin G, Mignot J and Menary M 2021 On the risk of abrupt changes in the north atlantic subpolar gyre in CMIP6 models *Ann. New York Acad. Sci.* **1504** 187–201
Ukkola A M, De Kauwe M G, Roderick M L, Abramowitz G and Pitman A J 2020 Robust future changes in meteorological drought in CMIP6 projections despite uncertainty in precipitation *Geophys. Res. Lett.* **47** e2020GL087820
Wang B and Ding Q 2006 Changes in global monsoon precipitation over the past 56 years *Geophys. Res. Lett.* **33** L06711
Wang B, Jin C and Liu J 2020 Understanding future change of global monsoons projected by CMIP6 models *J. Clim.* **33** 6471–89
Wang B, Kim H J, Kikuchi K and Kitoh A 2011 Diagnostic metrics for evaluation of annual and diurnal cycles *Clim. Dyn.* **37** 941–55
Watanabe M, Dufresne J L, Kosaka Y, Mauritsen T and Tatebe H 2021 Enhanced warming constrained by past trends in equatorial pacific sea surface temperature gradient *Nat. Clim. Change* **11** 33–37
Wilcox L J *et al* 2020 Accelerated increases in global and asian summer monsoon precipitation from future aerosol reductions *Atmos. Chem. Phys.* **20** 11955–77
Willmott C J and Feddema J J 1992 A more rational climatic moisture index* *Prof. Geogr.* **44** 84–88
Yang Y, Roderick M L, Zhang S, McVicar T R and Donohue R J 2019 Hydrologic implications of vegetation response to elevated CO_2 in climate projections *Nat. Clim. Change* **9** 44–48
Zarch M A, Sivakumar B, Malekinezhad H and Sharma A 2017 Future aridity under conditions of global climate change *J. Hydrol.* **554** 451–69